Design, Synthesis, Spectral analysis, Drug likeness prediction, and molecular docking investigations of new naphtho[2,1-b]furan encompassing pyrimidines as potential antimicrobial agents

Roopa D. L (dlroopacta@gmail.com)
N.M.K.R.V. College for Women
Basavarajaiah Suliphuldevara Mathada
Vijaya College
Punarva H. B
Indian Institute of Science

Research Article

Keywords: Drug-likeness prediction, Molecular Docking, Naphthofuran, Pyrimidine, and SAR study

Posted Date: February 1st, 2023

DOI: https://doi.org/10.21203/rs.3.rs-2525515/v1

Abstract

In view of the extremely important biological and medicinal properties of napthofurans, the synthesis of these heterocycles has fascinated the interest of medicinal and organic chemists. Keeping this in mind, we herein reporting synthesis, and antimicrobial evaluation of 4-N-aryl -naphtho[2,1-b]furo[3,2-d] pyrimidines 5 (a-l). Structures of these synthesized compounds were confirmed by spectral analysis like IR, NMR and Mass spectrometry. The In vitro antimicrobial activities were reported for the all compounds 5 (a-l). The compounds 5e and 5f exhibited excellent antibacterial, antifungal and antidermatophytic activities against tested pathogens at MIC 3.125, and 3.125g/ml respectively. Furthermore, molecular docking studies of these compounds against Staphylococcus aureus tyrosyl-tRNA synthetase (PDB ID: 1JIJ), S. Aureus Gyrase (PDB ID: 2XCT) and SARS-CoV-2 Omicron (PDB ID: 7TOB), revealed the potential binding mode of the ligands to the site of the appropriate targets. Finally, drug likeness and structures activity relationship studies also disclosed.

Introduction

The quick emergence of resistant bacteria is happening worldwide, imperiling the worth of antibiotics, which have converted medicine and saved millions of lives [1]. A group of multidrug resistance bacteria collectively known as “ESKAPE”, which includes Gram-positive and Gram-negative, are often isolated in hospital atmospheres, where they are accountable for the common of nosocomial contagions [2].

Several heterocyclic motifs signify an important family of naturally products and synthetic molecules that are distinguished for their biological activities [3–7].The pyrimidine derivatives encompass an assorted and interesting group of drugs and very well known in medicinal chemistry for their therapeutic applications. They play important role as anti-convulsant [8], antibacterial [9], cardiovascular [10], treatment of viral infection [11], anti-inflammatory [12], and anti-cancer [13] drugs and are connected with various biodynamic properties, noticed in the context of drug design and development. Furthermore, the furo[3,2-*d*]pyrimidine derivatives were reported as inhibitors of dihydrofolate reductase [14]. The derivatives of naphtho[2,1-*b*]furan acquire different biological and pharmacological activities, such as anthelmintic, antibacterial, anti-inflammatory, antifungal, analgesic and antineoplastic activities [15–20].

Several furan and pyrimidine derived drugs are accessible in the market [**Figure-1**], in continuation of our research interest on synthesis and biological activities of heterocycles [21–28] and which were encourage our interest to investigate a series of N-(4-chlorophenyl)naphtho[1',2':4,5]furo[3,2-d]pyrimidin-8-amines **5(a-l)** compounds and examine their binding interaction with microorganisms by the molecular docking method. To categorize possible drug candidates, the newly synthesized compounds were tested for their antimicrobial activity. The structures of synthesised compounds were characterised by IR, NMR and mass spectral analysis.

Results And Discussion

Chemistry

As a result of proper functionalization of naphtho[2,1-*b*]furans, substituted naphtho[2,1-*b*]furo[3,2-*d*]pyrimidine derivatives are synthesized. For the preparation of naphthofuro-pyrimidines, ethyl-3-amino naphtho[2,1-*b*]furan-2-carboxylate **2** is necessary, which is synthesized from 2-hydroxy-1-naphthonitrile **1**. In the presence of a base, K_2CO_3, we cycled 2-hydroxy-1-naphthonitrile **1** with ethyl chloroacetate to produce ethyl 3-amino naphtho[2,1-b]furan-2-carboxylate **2**. While the reaction was being observed by TLC in the mobile phase of hexane:ethyl acetate, excellent yields of the final product were produced. To ensure purity and identity, the product underwent column chromatography purification, NMR identification, and mass spectrometry confirmation. In the IR spectrum of compound **2**, there are bands at 3426 and 1657 cm^{-1} that correspond to the stretching of NH_2 and ester carbonyl, respectively. The presence of a δCH_3 proton and a δCH_2 proton of the ethyl group are indicated by a triplet at 1.4 and a quartet at 4.4, respectively, in the ^1H NMR spectra. A singlet at δ6.48 owing to NH_2 further supports the production of the ethyl amino ester of naphthofuran.

By heating compound **2** with formamide, the compound was further condensed and cyclized to provide a quantifiable yield of 4-oxo-naphtho[2,1-b]furo[3,2-d]pyrimidine **3**. The spectroscopic approach was used to characterize the compound **3**.The IR spectra revealed a broad carbonyl stretching frequency at 1678 cm^{-1} and a strong absorption band at 3393 cm^{-1} attributed to the -NH group. The compound had indeed synthesized, as evidenced by the decrease in carbonyl stretching frequency from 1708 cm^{-1} to 1678 cm^{-1}. The distinctive new singlet signal was visible in the ^1H NMR spectrum at δ13 to -NH proton. The molecular ion peak M + 1, which was recorded at 237, could be seen in the mass spectra.

Compound **3** was heated with phosphorous oxychloride to create 4-chloro-naphtho[2,1-b]furo[3,2-d]pyrimidine **4**. The compound **4** was formed, as shown by the absence of stretching bands in its IR spectrum caused by the carbonyl and -NH groups. The compound's synthesis was verified by the IR spectrum's absorption band at 811 cm^{-1} caused by the C-Cl bond.

The 4-chloro naphtho[2,1-b]furo[3,2-d]pyrimidine **4** was given a nucleophilic substitution reaction alongside various aromatic amines in order to produce a type of 4-amino substitutednaphtho[2,1-*b*]furo[3,2-*d*]pyrimidine **5 (a-l)** descendants and learn more about the effects of different substituent types on the biological activity of napthofuran pyrimidine. On the basis of spectral data, the structures of the produced compounds were verified. The IR spectra of **5f** showed absorption bands at 1629 cm^{-1} from the -C = N group and at 3394cm^{-1} from the -NH group. A singlet at position δ13 in the ^{1}H NMR spectrum was assigned to the -NH proton, and a multiplet for eleven aromatic protons was assigned to positions δ7.5 to δ 9.3 in the spectrum. Recording the mass spectrum further validated the compound's production, showing a molecular ion peak at m/z 356 (38%).

Antimicrobial Activities

The results antibacterial activity of synthesized derivatives exposed that the derivatives **5e, 5f**, and **5l** excellent potential to bacterial inhibition against *S. aureus*, with a MIC of 3.125 µg/ml and equal to the standard drug Gentamycin. The compounds **5d, 5g, 5i**, and **5j** showed good activity under same condition. The antibacterial activity of the rest of the compounds against *S. aureus* was moderate to less. Compounds **5e**, and **5f** had outstanding inhibition activity against *E. coli*, with MIC 3.125µg/ml, which is alike to the Gentamycin drug. Compounds **5d, 5i**, and **5l** showed activity against *E. coli* with a MIC of 6.25µg/ml, which was comparable to the standard drug. The remaining compounds have less to reasonable bacterial inhibition against the tested pathogens. Compounds **5e** & **5l** have elevated antibacterial activity against *S. typhi* (MIC 3.125 µg/ml) under same condition standard drug exhibited bacterial growth inhibition at same concentration. The compounds **5d, 5f, 5i**, and **5j** restrain the bacterial growth at 6.25 mg/ml. The left over compounds have been exhibited little to sensible inhibitory activity against *S. typhi* (**Table-1**).

Table-3: Antimicrobial activity results of the novel compounds (5a-l).

Compounds	Antibacterial activity in MIC (µg mL^{-1})			Antifungal activity in MIC (µg mL^{-1})			Antidermatophytic in MIC (µg mL^{-1})	
	S. aureus	*E. coli*	*S. typhi*	*C. albicans*	*A. Flavus*	*A. niger*	*T. rubrum*	*M. gypsyum*
5a	50	50	50	50	50	50	50	50
5b	50	50	50	100	100	50	100	100
5c	50	50	50	50	50	50	50	50
5d	6.25	6.25	6.25	6.25	6.25	6.25	6.25	6.25
5e	3.125	3.125	3.125	6.25	3.125	3.125	3.125	3.125
5f	3.125	3.125	6.25	6.25	3.125	3.125	3.125	3.125
5g	25	50	25	25	25	25	50	50
5h	50	50	50	50	50	50	50	50
5i	6.25	6.25	6.25	12.50	6.25	6.25	6.25	6.25
5j	6.25	6.25	6.25	12.50	6.25	6.25	6.25	6.25
5k	25	50	25	25	25	25	50	50
5l	3.125	6.25	3.125	6.25	3.125	3.125	6.25	6.25
Gentamycin	3.125	3.125	3.125					
Fluconazole				3.125	3.125	3.125		
Clotrimazole							3.125	3.125

The results of antifungal activity exposed that the compounds **5d, 5e, 5f**, & **5l** offered outstanding inhibition fungal growth against *C. albicans* with MIC 6.25 µg/ml, which is comparable to the standard drug at 3.125 µg/ml. The compounds **5i** and **5j** showed inhibitory activity at the concentration 12.50 µg/ml. The remaining derivatives showed less to medium action. The compounds **5d, 5i**, and **5j** showed very good activity with MIC 6.25 µg/ml against *A. flaus*. The rest of the molecules demonstrated less fair activity (**Table-1**).

The results of antidermatophytic activity showed that the compounds **5e**, & **5f** exhibited excellent inhibition activity against pathogens *T. rubrum* and *M. gypsyum* at concentration 3.125 µg/ml which is equal standard drug Clotrimazole. The compounds **5d, 5i**, and **5j** showed good inhibition activity at the concentration 6.25µg/ml against both the organisms and rest of the compounds exhibited less to moderate inhibitory activity. The antimicrobial activities results were tabulated in **Table-1**.

Molecular Docking Studies

Molecular docking of compounds 12 newly designed molecules and Ampicillin as the reference standard was performed to identify the ligand conformation with the best binding properties and most stability against *S. aureus TyrRS* (**PDB ID: 1JIJ**) protein. Bioinformatics analysis revealed that compounds **5a**, **5e**, and **5f** had the best binding interactions with *S. aureus TyrRS*. compound **5a** formed one hydrogen bond with Asp195 amino acids while Compound **5e** was observed to be bound to *S. aureus TyrRS* protein through the formation of two hydrogen bonds with Lys84 and Ser194 amino acids and compound **5f** formed two hydrogen bonds with Thr42 and His50 amino acids.

The **table-2** shows that compounds **5a, 5e**, and **5f** were stabilized inside the binding pocket of *S. aureus TyrRS* (**PDB ID: 1JIJ**) with very promising binding scores of -7.6, -8.2, and – 7.9 kcal/mol, respectively, compared to that of Ampicillin (-5.6 kcal/mol). The confirmation of Ampicillin formed 4 hydrogen bonds with Thr42, Arg88, His50, and His47 with distances 2.91, 2.94, 3.02, and 3.31Å, respectively; Out of the three best-synthesized ligands, the compound **5e** had the best binding energy, rmsd, and better interactions compared to **5a**, **5f**, and Ampicillin molecules (Figure: 2–5).

Table-2: Results of docking studies of compounds with S. aureus **TyrRS.**

Compound	UFF	Vina Score*	RMSD_UB	RMSD_LB	Hydrogen_bonds	Hydrogen_bond_distance*	Hydrophobic_bonds
5a	517.7	-7.6	4.941	5.171	['ASP195']	['3.07']	'THR42', 'HIS47', 'GLY49', 'HIS50', 'ASP195', 'PRO222', 'LEU223', 'VAL224', 'TRP241'
5e	495.82	-8.2	0	0	['LYS84', 'SER194']	['3.15', '3.20']	'ASP195', 'GLY83', 'SER82', 'LYS84', 'SER194', 'ASP153', 'TRP197'
5f	488.25	-7.9	7.282	9.541	['THR42', 'HIS50']	['3.16', '3.30']	'SER82', 'GLY83', 'LYS84', 'ASP153', 'SER194', 'ASP195', 'TRP197'
Amp	1066.66	-5.6	3.289	4.512	['THR42', 'ARG88', 'HIS50', 'HIS47']	['2.91', '2.94', '3.02', '3.31']	LYS84', 'THR42', 'ARG88', 'GLY49', 'LEU223', 'ASP195'

Molecular docking of compounds 12 newly designed molecules and Ampicillin as the reference standard was performed to identify the ligand conformation with the least binding energy and most stability against *S. aureus Gyrase* (**PDB ID: 2XCT**) proteins. Bioinformatics analysis revealed that compounds **5e, 5f**, and **5j** had the best binding interactions with *S. aureus Gyrase*. Compound **5f** was observed to be bound to *S. aureus Gyrase* protein through the formation of two hydrogen bonds with Arg1033, and Arg1048 amino acids while Compound **5e** formed one hydrogen bond with Arg1048 amino acid and compound **5j** from one hydrogen bond with Arg1048 amino acid.

The **table-3** shows that compounds **5e, 5f**, and **5j** were stabilized inside the binding pocket of *S. aureus Gyrase* (**PDB ID: 2XCT**) with very promising binding scores of -8.3, -8.5, and – 8.3 kcal/mol, respectively, compared to that of Ampicillin (-6.4 kcal/mol). Ampicillin formed 3 hydrogen bonds with Asp1148, Arg1048, and Ser1028 with distances 2.79, 2.88, and 3.20 Å, respectively. Out of the three best-synthesized ligands, compounds **5f** had the best binding energy, interactions and rmsd values compared to **5e, 5j**, and Ampicillin molecules (Fig. 6–9).

Table-3: Results of docking studies of synthesized compounds with S. aureus Gyrase.

Compound	UFF	Vina Score*	RMSD_UB	RMSD_LB	Hydrogen_ bonds	Hydrogen_ bond_distance*	Hydrophobic_bonds
5e	495.82	-8.3	0	0	['ARG1048']	['3.02']	['ASP510', 'GLY582', 'SER1028', 'ALA1032', 'ARG1033', 'ARG1048' ,'PRO1080', 'HIS1081', 'TYR1150']
5f	488.25	-8.5	0	0	['ARG1033', 'ARG1048']	['3.00', '2.83']	['ASP510', 'VAL511', 'ASP512', 'GLY582', 'SER1028', 'ALA1032', 'ARG1033', 'HIS1079', 'PRO1080', 'HIS1081']
5j	488.09	-8.3	0	0	['ARG1048']	['3.11']	['ASP510', 'GLY582', 'SER1028', 'ALA1032', 'ARG1033', 'ARG1048', 'PRO1080', 'HIS1081', 'TYR1150']
Amp	1066.66	-6.4	3.511	5.792	['ASP1148', 'ARG1048', 'SER1028']	['2.79', '2.88', '3.20']	['ALA509', 'ASP510', 'VAL511', 'ARG1048', 'PRO1080', 'HIS1081', 'ILE1147', 'ASP1148', 'ASN1149', 'TYR1150']

Molecular docking of compounds 12 newly designed molecules and Ampicillin as the reference standard was performed to identify the ligand conformation with the best binding properties and most stability against SARS-CoV-2 Omicron protein. Bioinformatics analysis revealed that compounds **5e, 5i**, and **5g** had the best binding interactions with SARS-CoV-2. Compound **5g** was observed to be bound to Protease (Mpro) protein through the formation of one hydrogen bond with Glu166 amino acid while Compound **5i** formed two hydrogen bonds with Glu166 amino acid and compound **5e** formed three hydrogen bonds with Glu166, Gly143, and His41 amino acids.

The **table-4** shows that compounds **5e, 5g**, and **5i** were stabilized inside the binding pocket of Protease (Mpro) of SARS-CoV-2 Omicron (**PDB ID: 7TOB**) with very promising binding scores of -8.8, -8.7 and − 8.6 kcal/mol, respectively, compared to that of Ampicillin (-6.5 kcal/mol). Ampicillin formed 1 hydrogen bond with Glu166, with a distance of 2.84 Å. Out of the four best-synthesized ligands, the compound **5g** had the best binding energy, rmsd, and better interactions compared to 5e, 5i, and Ampicillin molecules (Fig. 10–13).

Table-4: Results of docking studies of synthesized compounds with SARS-CoV-2 Omicron.

Compound	UFF	Vina Score*	RMSD_UB	RMSD_LB	Hydrogen_bonds	Hydrogen_bond_distance*	Hydrophobic_bonds
5e	495.82	-8.6	0	0	['GLY143', 'HIS41', 'GLU166']	['3.04', '3.05', '3.28']	'HIS41', 'LEU141', 'ASN142', 'GLY143', 'CYS145', 'MET165', 'GLU166', 'GLN189', 'THR190'
5g	481.04	-8.8	0	0	['GLU166']	['3.13']	['HIS41', 'MET49', 'LEU141', 'ASN142', 'CYS145', 'PHE140', 'HIS164', 'MET165', 'GLU166', 'ARG188', 'GLN189']
5i	477.97	-8.7	0	0	['GLU166', 'GLU166']	['3.06', '3.15']	'HIS41', 'LEU141', 'ASN142', 'GLY143', 'CYS145', 'MET165', 'GLU166', 'GLN189', 'THR190'
Amp	1090.55	-6.5	2.827	7.82	['GLU166']	['2.84']	'HIS41', 'MET165', 'GLU166', 'PRO168', 'ASP187', 'ARG188', 'GLN189', 'ALA191',

Drug-likeness Prediction

The physiochemical characteristics, ADMET, drug-likeness, and bioactivity scores for molecules are critical in their fundamental unique proof as a synthetic lead and serve as a baseline against which integrated compounds are tested during lead development. The http://www.swissadme.ch/

was used to screen the stages of absorption, distribution, metabolism, and excretion of all the synthesized molecules. The main goal of this study is to estimate the pharmacokinetic characteristics of the substances under investigation. **Table-5** showed the expected drug-likeness profiles of freshly synthesized compounds, as well as ADMET characteristics [29, 30].

Table-5: Physiochemical parameters of compounds 5a-l predicted by SwissADME.

Parameters*	5a	5b	5c	5d	5e	5f	5g	5h	5i	5j	5k	5l
MW	311.34	345.78	390.23	329.33	356.33	356.33	380.23	341.36	325.36	355.35	368.39	391.4
NHA	24	25	25	25	27	27	26	26	25	27	28	28
NAHA	23	23	23	23	23	23	23	23	23	23	23	23
NRB	2	2	2	2	3	3	2	3	2	3	4	3
NHBA	3	3	3	4	5	5	3	4	3	5	4	6
NHBD	1	1	1	1	1	1	1	1	1	2	2	2
MR	96.36	101.37	104.06	96.32	105.18	105.18	106.38	102.85	101.33	103.32	110.67	106.22
TPSA	5095	50.95	50.95	50.95	96.77	96.77	50.95	60.18	50.95	88.25	80.05	113.7
iLOGp	3.13	3.43	3.53	3.27	2.89	2.84	3.58	3.45	3.38	2.74	3.09	2.03
Log S (ESOL)	-5.6	-6.17	-6.49	-5.74	-5.63	-5.63	-6.76	-5.64	-5.88	-5.42	-5.2	-5.13
MLOGP	3.37	3.86	3.97	3.75	3.15	3.15	4.35	3.03	3.59	1.85	2.77	2.68
GI	High	High	High	High	High	High	High	High	High	High	High	High
BBBP	Yes	Yes	Yes	Yes	No	No	Yes	Yes	Yes	No	No	No
vLROF	0	0	0	0	0	0	1	0	0	0	0	0
vGR	0	1	1	1	1	1	1	0	0	0	0	1
vVR	0	0	0	0	0	0	0	0	0	0	0	0
BS	0.55	0.55	0.55	0.55	0.55	0.55	0.55	0.55	0.55	0.56	0.55	0.56
SA	3.17	3.13	3.2	3.11	3.24	3.36	3.18	3.16	3.15	3.06	3.26	3.29

*MW: Molecular weight; NHA: Num. heavy atoms; NAHA: Number of aromatic heavy atoms; NRB: Num. rotatable bonds; NHBA: Num. H-bond acceptors; NHBD: Num. H-bond donors; MR: Molar Refractivity; TPSA: Topological Polar Surface Area; Log S: Solubility class; MLOGP: Moriguchioctanol-water partition coefficient: GI: Gastrointestinal absorption; BBBP: Blood Brain Barrier Penetration; vLROF: Violation of Lipinski's rule of five; vGR: Violation of Ghose rule; vVR: Violation of Veber rule; BS: Bioavailability Score; SA: Synthetic accessibility.

Materials And Methods

Instrumentation

On a Perkin-Elmer FT-IR spectrophotometer (Spectrum ONE), (ν_{max} in per centimetre, KBr) were documented, ^{1}H (400 MHz) and ^{13}C NMR (100 MHz) spectra were documented on a Bruker AMX spectrophotometer using DMSO-d_6 as solvent and TMS as an internal standard ESI-mass was recorded on a mass spectrometer equipped with an electrospray ionization source having mass a range of 4000 amu in quadruple and 20,000 amu in Tof. The purity of the compounds was checked using TLC (silica gel 60G F254 plates) and iodine vapours were utilized as visualizing agents. The elemental analysis was carried out using the elemental analyzer Flash EA1112 series.

Experimental

The chemicals used in the experiments were procured from certified suppliers and used without further purification. The compounds **2–4** were synthesized according to literature methods [31, 32] and structures of these newly synthesized compounds matching with literature spectral data.

Synthesis of ethyl 3-aminonaphtho [2,1- b **]furan-2-carboxylate 2**:

Equimolar quantities of ethyl chloroacetate(2.46 g, 0.02 mol) and 2-hydroxy-1-naphthonitrile **1** (3.26 g, 0.02 mol) were combined and refluxed for three hours in 25 ml of dry acetonitrile with anhydrous potassium carbonate (0.02 mol). The reaction mixture was filtered and evaporated under vacuum to create the solid product, which was then purified using column chromatography.

Pale yellow crystals; yield: 80%; m. p. 79°C. IR(KBr) υ (cm^{-1}) : 3426(-NH_2), 1657(ester -C = O H bonded), 1164 (ring C-O-C); ^{1}H NMR (400 MHz, DMSO-d_6) δ = 1.4 (t, 3H, -CH_3), 4.4 (q, 2H, -CH_2), 5.4 (bs, 2H, -NH_2), 7.4–8.3 (m, 6H, ArH); ^{13}C NMR (100 MHz, DMSO–d_6) δ = 160.23, 134.07, 132.38, 131.44, 130.27, 129.82, 128.86, 128.56, 128.08, 127.84, 127.16, 125.65, 125.31, 59.23 and 18.45.MS (ESI): m/z (%): M + 255;Anal. Calcd for $C_{15}H_{13}NO_3$: C, 70.58; H, 5.13; N, 5.49. Found: C, 70.49; H, 4.90; N, 5.41%.

Synthesis of 4-oxo-naphtho[2,1- b **]furo[3,2-** d **]pyrimidine 3.**

The compound **2** (2.5 g, 0.01 mol) and formamide (10 ml) were heated together for 5 hrs. The separated solid product was filtered and re-crystallized using acetic acid. Light Green crystals; yield: 71%; m. p. 250°C. IR (KBr) υ (cm^{-1}): 3393(-NH), 1678(-C = O), 1623(-C = N); ^{1}H NMR (400 MHz, DMSO–d_6) δ = 13.0(s, 1H, -NH), 9.0(d, 1H, pyrimidine-CH), 7.5–8.4 (m, 6H, ArH); ^{13}C NMR (100 MHz, DMSO–d_6) δ = 154.56, 152. 23, 146.91, 144.72, 138.52, 131.09, 130.19, 128.87, 127.90, 127.71, 125.69, 123.63, 115.61, 113.09; MS (ESI): m/z (%): M + 1, 237 (48).Anal. Calcd for $C_{14}H_8N_2O_2$: C, 71.18; H, 3.41; N, 11.86. Found: C, 71.0; H, 3.30; N, 11.78%.

Synthesis of 4-chloro naphtho[2,1- b **]furo[3,2-** d **]pyrimidine (4).**

POCl3 (5 ml) and compound **3** (1 g) were refluxed for three hours, then put into ice cold water, separated by filtering, dried, and crystallised from ethanol. White solid; yield: 83%; m.p. 195°C. IR (KBr) υ (cm^{-1}) : 1606, 1577(-C = N), 811(C-Cl); ^{1}H NMR (400 MHz, DMSO–d_6) δ = 9.2(d, 1H, pyrimidine-CH), 7.6-9.0 (m, 6H, ArH); ^{13}C NMR (100 MHz, DMSO–d_6) δ = 155.16, 153. 13, 147.52, 143.82, 137.98, 130.89, 130.49, 129.27, 127.82, 126.96, 125.35, 124.03, 115.51, 112.59; MS (ESI): m/z (%): M^+, 254, 256 (100, 33); Anal. Calcd for $C_{14}H_7N_2OCl$: C, 66.03; H, 2.77; N, 11.00. Found: C, 65.80; H, 2.58; N, 10.90%.

General procedure for the synthesis of 4-arylaminonaphtho[2,1- b **]furo[3,2-** d **]pyrimidines 5(a-l).**

The compound **4** (0.5 g, 0.0022 mol) and appropriate amine (0.0022 mol) were refluxed in DMF (10 ml) for 5–6 hrs. After pouring the reaction mixture into ice-cold water, the solid fraction was filtered, dried, and purified using column chromatography.

4-Phenylamino naphtho[2,1- b **]furo[3,2-** d **]pyrimidines (5a).**

Yellow solid; yield: 96%; m.p. 125°C. IR(KBr) υ (cm^{-1}) : 1606 (–C = N), 3120 (-NH); ^{1}H NMR (400 MHz, DMSO–d_6) δ = 10.5(s, 1H, NH), 7.1 to 8.8 (m,12H, ArH); ^{13}C NMR (100 MHz, DMSO–d_6) δ = 154.56, 152.90, 152.23, 146.93, 144.72, 138.52, 133.12, 131.10, 130.20, 129.79, 128.88, 128.54, 127.92, 127.71, 125.71, 121.75, 113.10 and 109.85; MS (ESI): m/z (%): 312 (32%). Anal. Calcd for $C_{20}H_{13}N_3O$: C, 77.16; H, 4.21; N, 13.50. Found: C, 77.12; H, 4.18; N, 13.46%.

4-(4-Chlorophenylamino)-naphtho[2,1- b **]furo[3,2-** d **]pyrimidines (5b).**

Pale yellow solid; yield: 91%; m.p. 159°C. IR(KBr) υ (cm^{-1}) :835(-C-Cl), 1616 (–C = N), 3213 (-NH); ^{1}H NMR (400 MHz, DMSO–d_6) δ = 11.1(s, 1H, NH), 7.5 to 9.1 (m,11H, ArH); ^{13}C NMR (100 MHz, DMSO–d_6) δ = 156.31, 153.50, 152.91, 147.53, 145.72, 139.42, 137.82, 135.45, 134.60, 132.80, 130.79, 128.68, 128.64, 126.78, 126.10, 123.63, 114.13 and 111.45; MS (ESI): m/z (%): M^+, M + 2, 345, 347 (45, 15%). Anal. Calcd for $C_{20}H_{12}N_3OCl$: C, 69.47; H, 3.50; N, 12.15. Found: C, 69.42; H, 3.58; N, 12.08%.

4-(4-Bromophenylamino)- naphtho[2,1- b **]furo[3,2-** d **]pyrimidines (5c).**

Pale yellow solid; yield: 89%; m.p. 175°C. IR(KBr) υ (cm^{-1}) :620(-C-Br), 1656 (–C = N), 3090 (-NH); ^{1}H NMR (400 MHz, DMSO–d_6) δ = 11.3(s, 1H, NH), 7.4 to 9.3 (m,11H, ArH); ^{13}C NMR (100 MHz, DMSO–d_6) δ = 155.91, 154.50, 152.41, 147.63, 145.32, 139.72, 137.12, 135.85, 134.45, 132.25, 130.67, 128.55, 128.35, 126.97, 126.22, 123.56, 118.34 and 109.65; MS (ESI): m/z (%): M^+, M + 2, 390, 392 (18, 17%). Anal. Calcd for $C_{20}H_{12}N_3OBr$: C, 61.56; H, 4.10; N, 10.77. Found: C, 61.59; H, 4.06; N, 10.72%.

4-(4-Fluorophenylamino)- naphtho[2,1- b **]furo[3,2-** d **]pyrimidines (5d).**

Pale yellow solid; yield: 87%; m.p. 182°C. IR(KBr) υ (cm^{-1}) :1295(-C-F)1606 (–C = N), 3268(-NH); ^1H NMR (400 MHz, DMSO–d_6) δ = 11.5(s, 1H, NH), 7.3 to 9.1 (m,11H, ArH); ^{13}C NMR (100 MHz, DMSO–d_6) δ = 154.83, 154.10, 153.21, 146.23, 145.14, 138.32, 136.95, 134.85, 134.13, 132.53, 131.36, 128.88, 128.45, 126.58, 125.72, 123.67, 110.67 and 108.99; MS (ESI): m/z (%): 329 (42%). Anal. Calcd for $C_{20}H_{12}N_3OF$: C, 72.94; H, 3.67; N, 12.76. Found: C, 72.91; H, 3.69; N, 12.79%.

4-(4-Nitrophenylamino)- naphtho[2,1- b **]furo[3,2-** d **]pyrimidines (5e).**

Dark yellow solid; yield: 90%; m.p. 162°C. IR(KBr) υ (cm^{-1}) :1629 (–C = N), 3394 (-NH); ^1H NMR (400 MHz, DMSO–d_6) δ = 12.7(s, 1H, NH), 7.4 to 9.3 (m,11H, ArH); ^{13}C NMR (100 MHz, DMSO–d_6) δ = 153.89, 152.47, 151.12, 148.31, 146.11, 140.42, 139.74, 134.86, 133.30, 132.37, 131.29, 130.18, 129.54, 128.92, 127.98, 123.25, 114.60 and 112.05; MS (ESI): m/z (%): 356 (56%). Anal. Calcd for $C_{20}H_{12}N_4O_3$: C, 67.41; H, 3.39; N, 15.72. Found: C, 67.44; H, 3.41; N, 15.67%.

4-(3-Nitrophenylamino)- naphtho[2,1- b **]furo[3,2-** d **]pyrimidines (5f).**

Dark yellow solid; yield: 88%; m.p. 174°C. IR(KBr) υ (cm^{-1}) :1634 (–C = N), 3190 (-NH); ^1H NMR (400 MHz, DMSO–d_6) δ = 13.0(s, 1H, NH), 7.6 to 9.2 (m,11H, ArH); ^{13}C NMR (100 MHz, DMSO–d_6) δ = 155.42, 153.67, 151.89, 147.21, 145.02, 139.42,138.54, 133.82, 132.10, 131.12, 130.19, 129.38, 128.94, 128.32, 127.58, 127.58, 122.15, 116.12, 113.50 and 110.35; MS (ESI): m/z (%): 356 (38%). Anal. Calcd for $C_{20}H_{12}N_4O_3$: C, 67.41; H, 3.39; N, 15.72. Found: C, 67.38; H, 3.42; N, 15.78%.

4-(3,4-Dichlorophenylamino)- naphtho[2,1- b **]furo[3,2-** d **]pyrimidines (5g).**

Pale yellow solid; yield: 88%; m.p. 195°C. IR (KBr) υ (cm^{-1}) :1636 (–C = N), 3315(-NH); ^1H NMR (400 MHz, DMSO–d_6) δ = 13.2(s, 1H, NH), 7.6 to 9.4 (m,10H, ArH); ^{13}C NMR (100 MHz, DMSO–d_6) δ = 155.42, 154.67 153.67, 151.89, 147.21, 145.02, 138.54, 136.67, 135. 23, 134.52, 133.10, 132.32, 131.57, 128.88,, 127.12, 127.12, 123.15, 115.52, 114.10 and 109.15; MS (ESI): m/z (%): 380 (62%). Anal. Calcd for $C_{20}H_{11}N_3OCl_2$: C, 63.18; H, 2.92; N, 11.05. Found: C, 63.21; H, 2.95; N, 11.10%.

4-(4-Methoxyhenylamino)- naphtho[2,1- b **]furo[3,2-** d **]pyrimidines (5h).**

Yellow solid; yield: 94%; m.p. 144°C. IR(KBr) υ (cm^{-1}) :1634 (–C = N), 3245(-NH); ^1H NMR (400 MHz, DMSO–d_6) δ = 11.8(s, 1H, NH), 7.2 to 8.9 (m,11H, ArH),4.1(s, 3H, OCH_3); ^{13}C NMR (100 MHz, DMSO–d_6) δ = 153.83, 153.15, 152.41, 145.16, 144.56, 137.16, 135.75, 134.96, 134.34, 132.38, 132.56, 128.65, 128.13, 126.43, 125.85, 123.67, 112.23, 109.45 and 60; MS (ESI): m/z (%): 312 (28%). Anal. Calcd for $C_{20}H_{13}N_3O$: C, 73.89; H, 4.43; N, 12.31. Found: C, 73.92; H, 4.47; N, 12.28%.

4-(4-Methylphenylamino)- naphtho[2,1- b **]furo[3,2-** d **]pyrimidines (5i).**

Yellow solid; yield: 92%; m.p. 156°C. IR(KBr) υ (cm^{-1}) : 1624(–C = N), 3301(-NH); ^1H NMR (400 MHz, DMSO–d_6) δ = 12.3(s, 1H, NH), 7.2 to 9.1 (m,11H, ArH), 2.2(s, 3H, CH_3); ^{13}C NMR (100 MHz, DMSO–d_6) δ = 154.45, 153.27, 152.69, 146.53, 144.72, 139.54, 135.62, 134.82, 133, 85, 133.12, 132.47, 128.73, 128.34, 128.08, 127.32, 123.65, 116.32, 108.35; and 20.52; MS (ESI): m/z (%): 325 (61%). Anal. Calcd for $C_{21}H_{15}N_3O$: C, 77.52; H, 4.65; N, 12.91;. Found: C, 77.55; H, 4.61; N, 12.94%.

4-(Naphtho[2,1- b **]furo[3,2-** d **]pyrimidine-4yl)-amino benzoic acid (5j).**

Brown solid; yield: 91%; m.p. 152°C. IR(KBr) υ (cm^{-1}) :1710(-C = O), 1624 (–C = N), 3230(-OH) 3370(-NH); ^1H NMR (400 MHz, DMSO–d_6) δ = 13.2(s, 1H, -COOH), 12.5(s, 1H, NH), 7.6to 9.4 (m,11H, ArH); ^{13}C NMR (100 MHz, DMSO–d_6) δ = 171.02, 154.86, 154.37, 152.43, 147.65, 146.52, 140.72, 133.52, 132.90, 129.68, 129.44, 128.62, 127.85, 127.26, 127.35, 126.85, 122.35, 112.87 and 109.55; MS (ESI): m/z (%): 355 (52%). Anal. Calcd for $C_{21}H_{13}N_3O_3$: C, 70.98; H, 3.69; N, 11.83. Found: C, 70.91; H, 3.72; N, 11.88%.

4-(4-Acetamidophenylamino)- naphtho[2,1- b **]furo[3,2-** d **]pyrimidines (5k).**

Brown solid; yield: 86%; m.p. 183°C. IR(KBr) υ (cm^{-1}) :1695(-C = O), 1623 (–C = N), 3294(-NH); ^1H NMR (400 MHz, DMSO–d_6) δ = 13.5(s, 1H, -NHCO), 12.8(s, 1H, NH), 7.6 to 9.4 (m,11H, ArH), 2.8(s, 3H, CH_3); ^{13}C NMR (100 MHz, DMSO–d_6) δ = 169.86, 155.61, 154.68, 153.09, 147. 79,146. 32, 139.27, 132.38, 130.27, 129.36, 128.61, 128.33, 127.84, 125.79, 125.73, 124.02, 119.08, 117.27, 109.41 and 28.23; MS (ESI): m/z (%): 368 (74%). Anal. Calcd for $C_{20}H_{13}N_3O$: C, 71.73; H, 4.38; N, 15.21. Found: C, 71.73; H, 4.38; N, 15.21%.

4-(Naphtho[2,1- b **]furo[3,2-** d **]pyrimidine-4yl)-amino benzene sulfonic acid (5l).**

Dark Brown solid; yield: 88%; m.p. 220°C. IR(KBr) υ (cm^{-1}):1350 (-S = O), 1618 (–C = N), 3370(-NH), 3450(-OH);^{1}H NMR (400 MHz, DMSO–d_6) δ = 11.8(s, 1H, -SO_3H), 13.4 (s, 1H, NH), 7.6 to 9.3 (m,11H, ArH); ^{13}C NMR (100 MHz, DMSO–d_6) δ = 154.56, 153.57, 152.53, 147.65, 146.22, 139.82, 134.63, 132.73, 129.56, 129.36, 128.89, 127.65, 127.16, 126.85, 126.42, 122.87, 113.90 and 110.13; MS (ESI): m/z (%): 391 (18%). Anal. Calcd for $C_{20}H_{13}N_3O_4S$: C, 61.37; H, 3.35; N, 10.74. Found: C, 61.31; H, 3.30; N, 10.79%.

Antimicrobial Activity

The evaluation of antimicrobial activity of novel compounds 4-substituted-naphtho[2,1-b]furo[3,2-d]pyrimidines 5**(a-l)** by disc (Muller-Hinton) and well diffusion method (potato dextrose agar). The activities were performed at various concentrations (3.125, 6.25, 12.5, 25, 50 and 100 µg/ml in DMSO). The antibacterial activity was performed by MIC method against four bacteria: *S. aureus* (MTCC 3160), *E. coli* (MTCC 46) and *S. typhi* (MTCC 98), as well as antifungal activity against four fungi: *C. albicans* (MTCC 227), *A. flavus* (MTCC 1883), and *A. niger* (MTCC 1881). Further the antidermatophytic activities against *T. rubrum* and *M. gypsyum* were evaluated for all the synthesized compounds **5(a-l)**. The activity follows CLSI's international suggestion. The MIC for each strain is the lowest concentration of test substance that causes no observable growth of bacteria or fungus. The use of DMSO in the formulation of the test solution has been found to not affect the test organisms in blank tests. Gentamycin, Fluconazole and Clotrimazole drugs used for antibacterial, antifungal and antidermatophytic activity respectively, were used to compare the results under identical settings [33, 34].

1.1. Molecular docking studies

The three-dimensional (3D) protein structure of *S. aureus TyrRS* (**PDB ID: 1JIJ**), *S. aureus Gyrase* (**PDB ID: 2XCT**), and protease (Mpro) of *SARS-CoV-2 Omicron* (**PDB ID: 7TOB**) were obtained from Protein Data Bank. The ligand molecules were sketched using ChemDraw Ultra 12.0 and then converted into 3D structures by optimizing their partial charges. A molecular docking study of the 12 newly designed molecules and Ampicillin as the reference standard was performed using PyRX-0.9.2 software. The ligands were docked using the AutoDock Vina program to identify the compound with the best binding characteristics. For the protein S. aureus TyrRS the grid box was set to the XYZ coordinates as 29.843, 21.580, and 26.599, respectively, with the centers of XYZ in the positions of -10.817, 12.479, and 84.378, respectively. The grid box for the protein S. aureus Gyrase was set to the XZY coordinates of 34.518, 29.618, and 47.853, with the XYZ centers of 5.810, 61.473, and 68.054, respectively. Blind dicked was performed with protease protein of SARS-CoV2 Omicron, and the grid box was set to the XYZ coordinates as size 61.12, 65.12, 39.90, with the XYZ centers of -2.04, 0.47, and 12.78 respectively. The nine conformations of each compound, along with the Vina score and RMSD value, were used to screen for the best binding interaction. The interaction of the ligands was analyzed using the 2D interaction diagrams generated by using LigPlot + and 3D interaction images using PyMOL [35, 36].

Structure Activity Relationship Studies

4-Substitution-naphtho[2,1-b]furo[3,2-d]pyrimidine is combination of the hydrophobic napthofuran, bioactive pyrimidine ring and hydrophilic-NHR group makes this molecule a ideal motif to develop drug candidates. The derivitisation of amine group at 4 position of napthofuran-pyrimidine with various substituted aromatic functions resulting in to various compounds become selective inhibitors for growth of the microbial pathogens. The results clearly indicates activity increases with substitution of aromatic group having electron rich group and further the alkyl substitution less potent as compare to aromatic substation. The brief SAR for synthesized compounds highlighted in **figure-11**.

Conclusion

The design, synthesis and biological potential new heterocycles has gained more interest in the field of drug discovery and development. Furthermore, present scenario of research work, specify that napthofuran and pyrimidine hybrids have exposed various possible antimicrobial activity compared to standard drugs. In the continuation of our investigate we have synthesised novel napthofurans derived pyrimidines and evaluated for their antimicrobial activites by *In vitro* and *In silico* methods. The drug-likeness prediction studies were gave the excellent outcome for the synthesised compounds to become excellent drug candidates. Compounds **5e** and **5f** showed excellent inhibitory activity against all the tested microbial pathogens at MIC 3.125 µg/ml concentration. Further these compounds gave excellent docking score against proteins *S. aureus* TyrRS, *S. aureus* Gyrase and *SARS-CoV-2 Omicron*. From the structure activity relationship studies clearly indicates that the nitro aromatic substitutions showing better inhibitory activity against microbial pathogens.

Declarations

Conflict of Interests:

The authors report no conflict of interest.

Acknowledgment

The authors are indebted to The Directors of IISc, Bengaluru, SAIF Punjab University, and CDRI, Lucknow for spectral data. For biological activities, the authors are grateful to The Director, Skanda Life Sciences Pvt. Ltd., Bengaluru.

References

1. Ventola CL. (2015) The antibiotic resistance crisis: part 1: causes and threats. P T. 40(4): 277 – 83. PMID: 25859123; PMCID: PMC4378521.
2. Pisano MB, Kumar A, Medda R, Gatto G. et al (2019) Antibacterial Activity and Molecular Docking Studies of a Selected Series of Hydroxy-3-arylcoumarins. Molecules 1, 24(15) 2815–2821. doi: 10.3390/molecules24152815.
3. Matada BS, Pattanashettar R, Yernale NG (2021) A Comprehensive Review on the Biological Interest of Quinoline and its Derivatives. Bioorg. Med. Chem. 32: 115973. https://doi.org/10.1016/j.bmc.2020.115973
4. Jeelan Basha N, Basavarajaiah SM, Shyamsunder K (2022) Therapeutic potential of pyrrole and pyrrolidine analogs: an update. Mol Divers. https://doi.org/10.1007/s11030-022-10387-8
5. Jeelan Basha N, Basavarajaiah SM, Swathi B, Prasanna Kumar (2021) A comprehensive insight on the biological potential of embelin and its derivatives, Natural Product Research, DOI: 10.1080/14786419.2021.1955361
6. Basavarajaiah SM, Sasidhar BS (2022) An Insight into the Recent Developments in Anti-infective Potential of Indole and Associated Hybrids. J Mol Stru 132808 https://doi.org/10.1016/j.molstruc.2022.132808
7. Basavarajaiah SM (2022) The Versatile Quinoline and Its Derivatives as anti-Cancer Agents: An Overview, Polycyclic Aromatic Compounds, DOI: 10.1080/10406638.2022.2089177
8. Kumar S, Deep A, Narasimhan B. (2015) Pyrimidine derivatives as potential agents acting on central nervous system. Cent Nerv Syst Agents Med Chem 15(1): 5–10. doi: 10.2174/1871524914666140923130138
9. Mallikarjunaswamy C, Mallesha L, Bhadregowda DG, Othbert Pinto (2017) Studies on synthesis of pyrimidine derivatives and their antimicrobial activity, Arabian Journal of Chemistry, 10 (1): S484-S490,https://doi.org/10.1016/j.arabjc.2012.10.008
10. Irshad N, Khan AU, Alamgeer, Khan SU, Iqbal MS (2021) Antihypertensive potential of selected pyrimidine derivatives: Explanation of underlying mechanistic pathways. Biomed Pharmacother. 139: 111567. doi: 10.1016/j.biopha.2021.111567
11. Dongwei Kang, Heng Zhang, Zhao Wang, Tong Zhao et al (2019), Identification of Dihydrofuro[3,4-d]pyrimidine Derivatives as Novel HIV-1 Non-Nucleoside Reverse Transcriptase Inhibitors with Promising Antiviral Activities and Desirable Physicochemical Properties *Journal of Medicinal Chemistry 62* (3): 1484–1501. DOI: 10.1021/acs.jmedchem.8b01656
12. Patil PT, Warekar PP, Patil KT et al (2018) A simple and efficient one-pot novel synthesis of pyrazolo[3,4-b][1,8]naphthyridine and pyrazolo[3,4-d]pyrimido[1,2-a]pyrimidine derivatives as anti-inflammatory agents. Res Chem Intermed 44: 1119–1130. https://doi.org/10.1007/s11164-017-3155-5
13. Tylińska B, Wiatrak B, Czyżnikowska Ż, Cieśla-Niechwiadowicz A (2021) Novel Pyrimidine Derivatives as Potential Anticancer Agents: Synthesis, Biological Evaluation and Molecular Docking Study. Int J Mol Sci 7; 22(8): 3825. doi: 10.3390/ijms22083825
14. Aleem gangjee, Elfatih, Elzein, Sherry F, Queener and John J. Meguire (1998) Synthesis and Biological Activities of Tricyclic Conformationally Restricted Tetrahydropyrido Annulated Furo[2,3-d]pyrimidines as Inhibitors of Dihydrofolate Reductases, J. Med. Chem., 41: 1409–1416.
15. Vanita GK, Ramaiah M, Shashikaladevi K, Veena K et al (2010) Synthesis of urethanes and substituted ureas encompassing naphtho[2.1-b]furan and evaluation their analgesic activity J Chem Pharm Res 2(6): 258–264.
16. Chaitanya MS, Nagendrappa G and Vaidya VP (2010) Synthesis, biological and pharmacological activities of 2-methyl-4Hpyrimido[2,1-b][1,3]benzothiazoles, J Chem Pharm Res 2(3): 206–213.
17. Mruthyunjayaswamy BHM, Shanthaveerappa BK, Basavarajaiah SM (2010) Synthesis and antimicrobial activity of 5-substituted-2-phenyl-3-(o-carboethoxyphenyl) iminomethyl indoles and their derivatives. J of Indian Chem Soc 87(9): 1109–1115. http://dx.doi.org/10.1002/chin.201111132
18. Vagdevi HM and Vaidya V P. (2001) Studies in naphthofurans: Part III- synthesis of 2-substituted naphtho [2,1-b] furans, 2-(2'-aryl-3'-acetyl-1', 3', 4'-oxadiazolyl) aminonaphtho [2,1-b] furans and their biological activities Indian J Heterocyclic Chem 10: 253–260.
19. Srivastava V, Negi AS, Kumar JK, Faridi U (2006) Bio Org Med Chem. Lett. 16(4): 911–4.

20. Gao J, Chen Q-Q, Huang Y, Li K-H, et al (2021) Design, Synthesis and Pharmacological Evaluation of Naphthofuran Derivatives as Potent SIRT1 Activators Front. Pharmacol. 12:653233. doi: 10.3389/fphar.2021.653233.
21. Chandrashekhar C, Vaidya VP, Roop DL (2009) Synthesis of 3-nitro-2-(3 '-acetyl-2 '-aryl-2 ', 3 '-dihydro-1 ',3 ',4 '-oxadiazol-5 '-yl) aminonaphtho [2,1-b] furans and their biological activities, Indian Journal of Heterocyclic Chemistry 18(4): 373–376. https://www.webofscience.com/wos/WOSCC/full-record/000268471200014
22. Shashikala Devi K, Ramaiah M, Roopa DL, and Vaidya VP, (2010) Synthesis and Investigation of Antimicrobial and Antioxidant Activity of 3-Nitro-N- (3-chloro-2-oxo-substituted-phenyl-azetidin-1-yl)naphtho [2,1-b]furan-2-carboxamides, J. of Chemistry, 7; S358-S362. https://doi.org/10.1155/2010/863547
23. Matada BS, Yernale NG, The contemporary synthetic recipes to access versatile quinoline heterocycles Synth. Commun. 51 (2021) 1133–1159. DOI: 10.1080/00397911.2021.1876240.
24. Matada BS, Yernale NG (2021) Modern encroachment in synthetic approaches to access nifty quinoline heterocycles. J Indian Chem Soc 98: 100174. https://doi.org/10.1016/j.jics.2021.100174.
25. Mathada BS, Yernale NG, Basha NJ, Badiger J (2021) An insight into the advanced synthetic recipes to access ubiquitous indole heterocycles. Tetrahedron Lett 85: 153458. https://doi.org/10.1016/j.tetlet.2021.153458
26. Matada BS, Yernale NG, Javeed M (2021) Design, Spectroscopic Studies, DFT Calculations and Evaluation of Biological Activity of Novel 1,3-Benzoxazines Encompassing Isoniazid Polycycl Aromatic Compd DOI: 10.1080/10406638.2021.2019062
27. Basavarajaiah SM, Nagesh GY, Basha NJ (2021) Physical Sciences Reviews: 000010151520210040. https://doi.org/10.1515/psr-2021-0040
28. Mathada BS, Yernale NG and Basha JN (2023) The Multi-Pharmacological Targeted Role of Indole and its Derivatives: A review, *ChemistrySelect* 8 (2023) e202204181. doi.org/10.1002/slct.202204181
29. Daina A, Michielin O, and Zoete V, (2017) "SwissADME: a free web tool to evaluate pharmacokinetics, drug-likeness and medicinal chemistry friendliness of small molecules", *Scientific Reports* 7: 42717. https://doi.org/10.1038/srep42717.
30. Mathada BS, Basha NJ, Prashantha K, Ganga P, et al (2023) Investigation of embelin synthetic hybrids as potential COVID-19 and COX inhibitors: Synthesis, spectral analysis, DFT calculations and molecular docking studies, Journal of Molecular Structure, 1273: 134356. https://doi.org/10.1016/j.molstruc.2022.134356.
31. Kodihalli CR, Hosadu MV, Vijayvithal PV (2008) Synthesis and antimicrobial activity of novel naphtho[2,1-b]furo-5H-[3,2-d] [1,3,4]thiadiazolo[3,2-a]pyrimidin-5-ones Arkivoc (11): 1–10.
32. Badr MZA. Kamal El-Dean AM, Moustafa OS, Zaki RMJ (2007) One-Pot Synthesis of Pyrido[2,3-d]Pyrimidine-2-Thiones and a Study of Their Reactivity Towards Some Reagents Chin. Chem. Soc. 54(4): 1045–1052.
33. Nagesh GY, Mohammad J, Jeelan NB, Prashantha K et al et al (2022) Design, Spectral analysis, DFT calculations, antimicrobial, anti-TB, antioxidant activity and molecular docking studies of novel bis-benzoxazines with cytochrome c peroxidase, Journal of Molecular Structure, 1262: 132977, https://doi.org/10.1016/j.molstruc.2022.132977.
34. Basavarajaiah SM, Nagesh GY, Javeed M, Bhat R et al (2022) "Synthesis, spectral analysis, DFT calculations, biological potential and molecular docking studies of indole appended pyrazolo-triazine", Molecular Diversity https://doi.org/10.1007/s11030-022-10448-y.
35. Basavarajaiah SM, Mruthyunjayaswamy BHM (2018) Synthesis and anti-microbial activity of (Z)-4-(4-substituted-thiazol-2-yl)-l-(2-oxoindolin-3-ylidene) semicarbazide and its derivatives. Indian J. Chemistry, 48B (10): 1274–1278.
36. Basavarajaiah SM, Mruthyunjayaswamy BHM (2009) Synthesis and anti-microbial activity of some new 5-substituted-n1-[(1e)-(2-hydroxyquinolin-3-yl)methylene]-3-phenyl-1h-indole-2-carbohydrzide derivatives. Hetero Comm 15(3): 217–224. https://doi.org/10.1515/HC.2009.15.3.217
37. DeLano, W. L. (2002). PyMOL
38. Laskowski RA and Swindells MB (2011). LigPlot+: multiple ligand–protein interaction diagrams for drug discovery.

Scheme

Scheme 1 is available in Supplementary Files section.

Figures

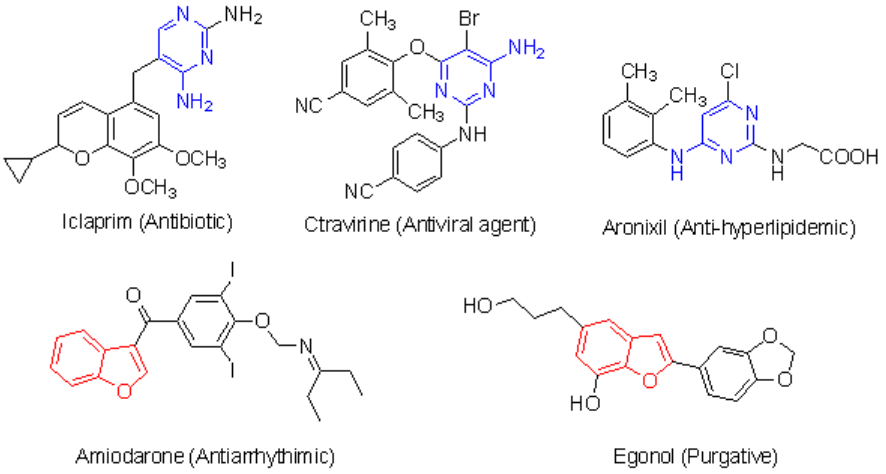

Figure 1

Examples of drug molecule containing pyrimidine and benzofurans motif.

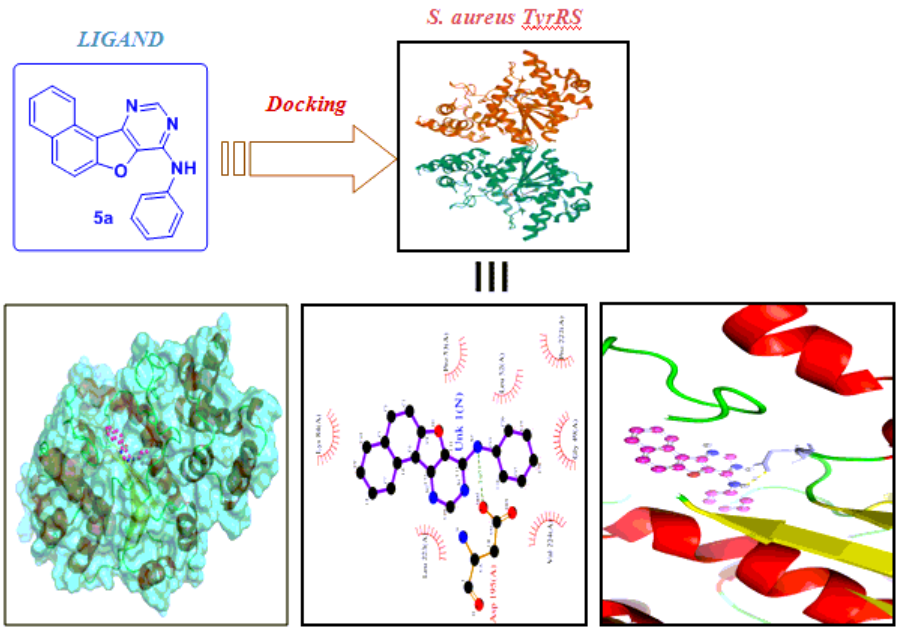

Figure 2

Docking studies of compound 5a with *S. aureus*TyrRS.

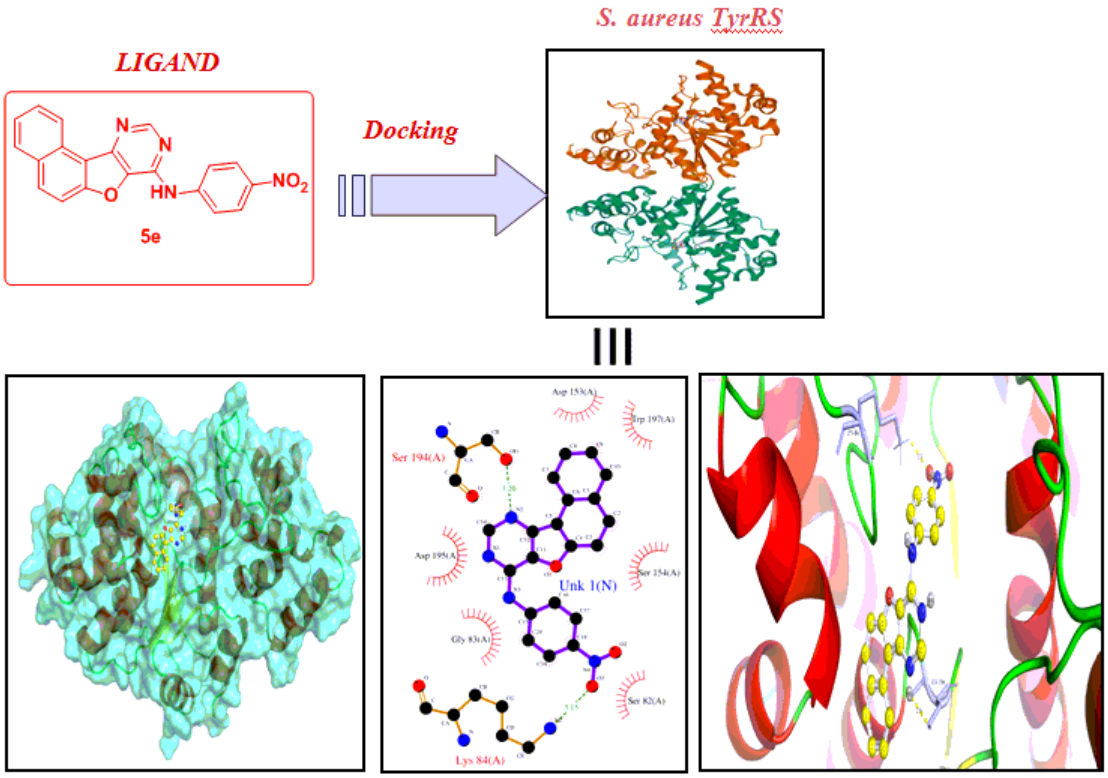

Figure 3

Docking studies of compound 5e with *S. aureus*TyrRS

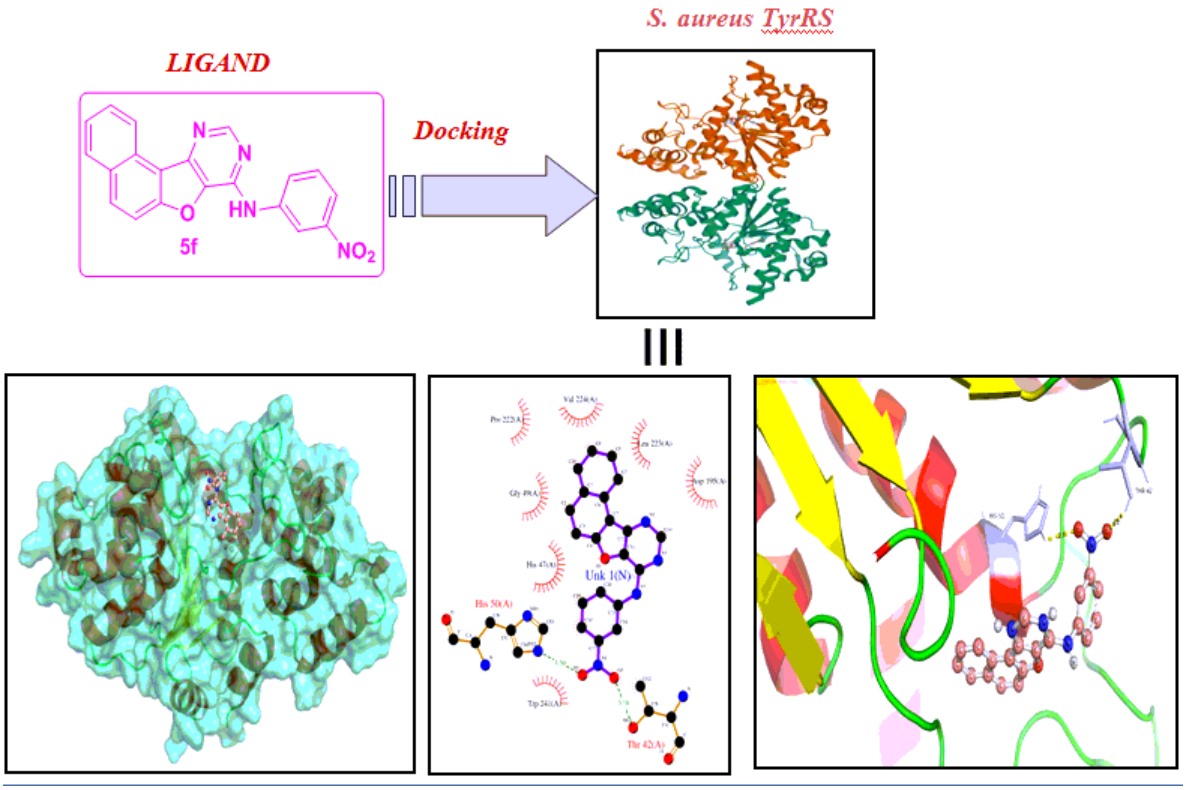

Figure 4

Docking studies of compound 5f with *S. aureus*TyrRS

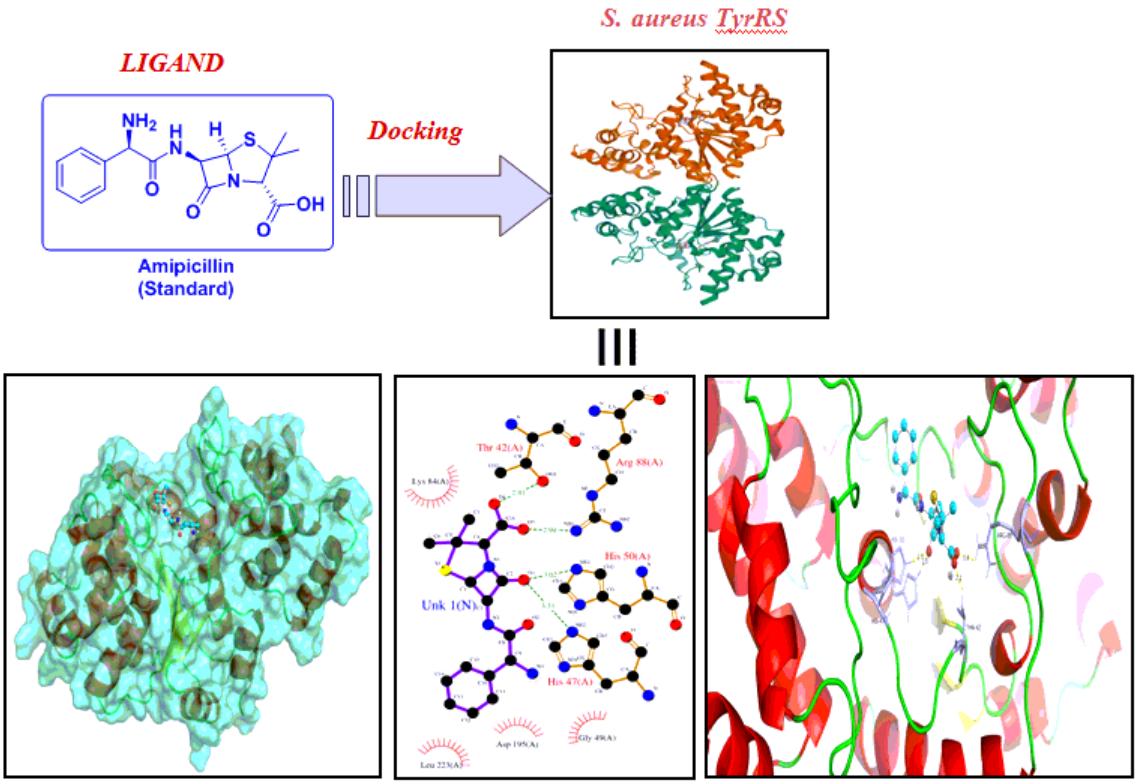

Figure 5

Docking studies of Ampicillin with *S. aureus*TyrRS

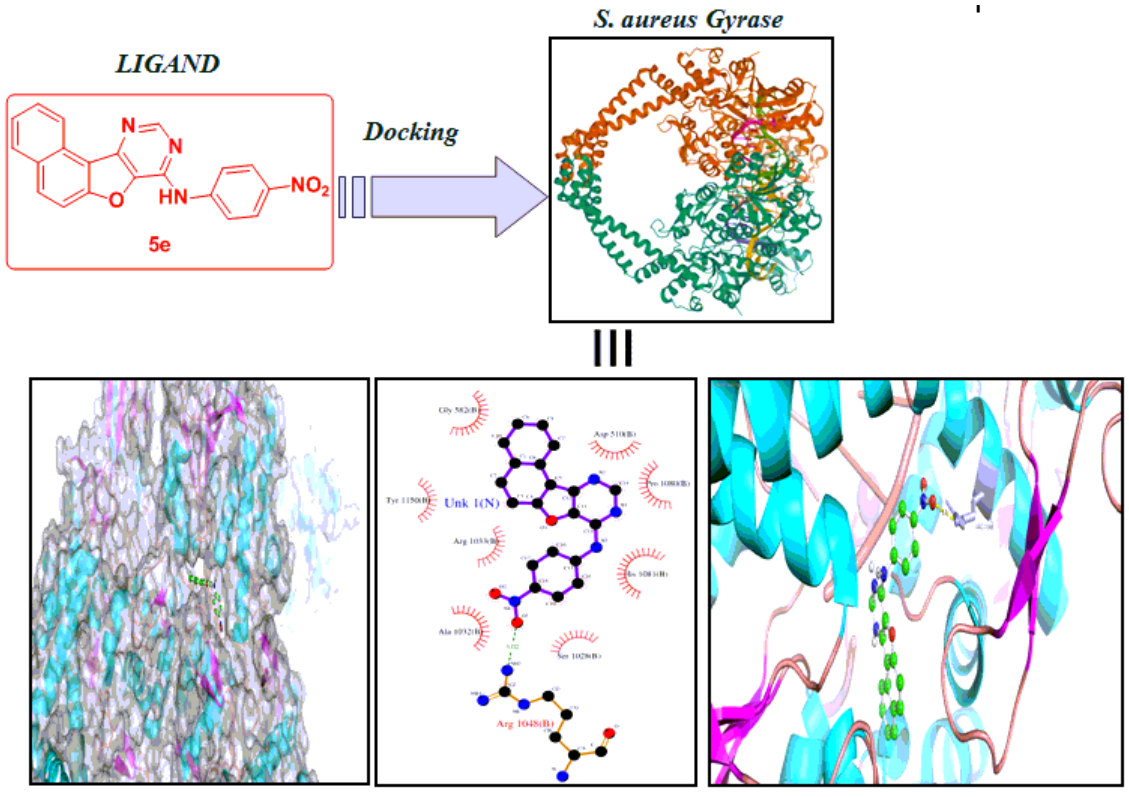

Figure 6

Docking studies of compound 5e with *S. aureus Gyrase*

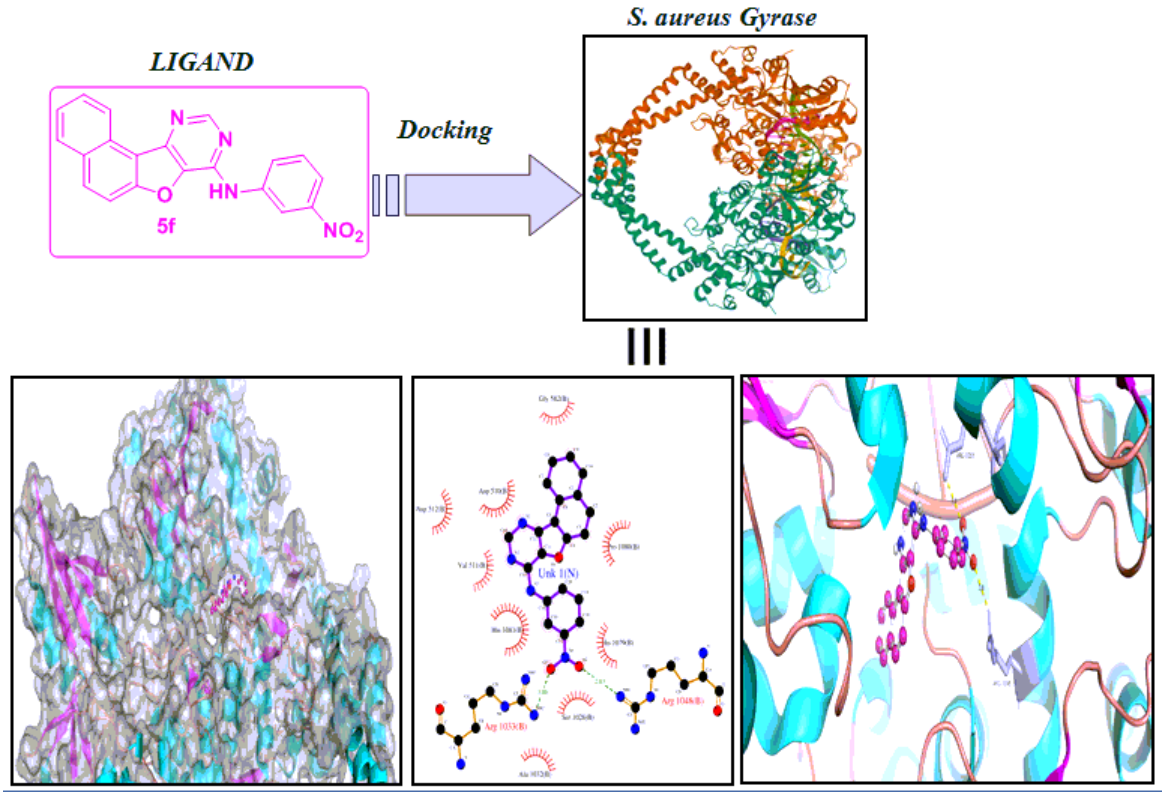

Figure 7

Docking studies of compound 5f with *S. aureus Gyrase*

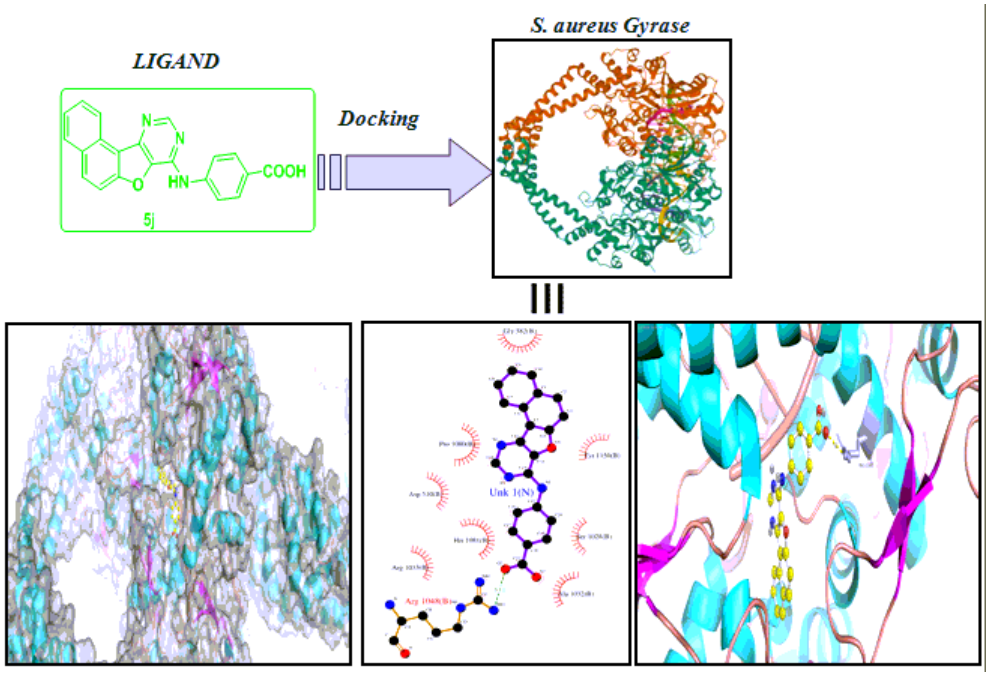

Figure 8

Docking studies of compound 5j with *S. aureus Gyrase*

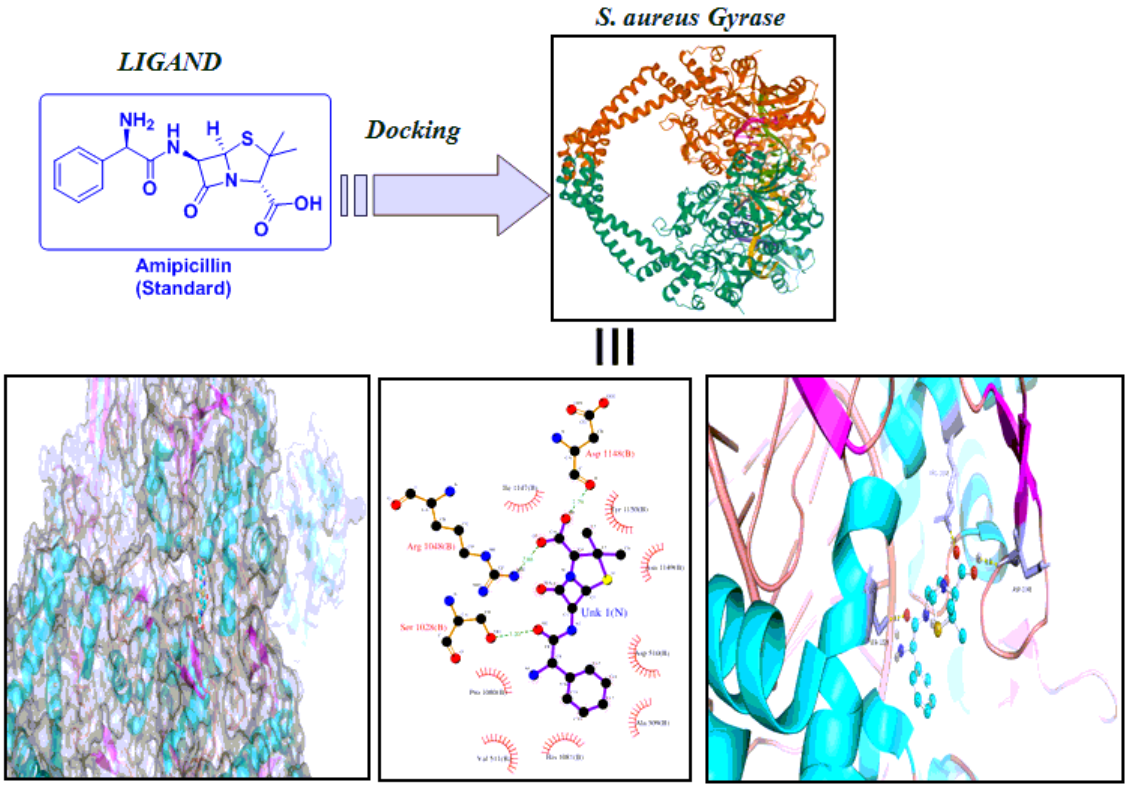

Figure 9

Docking studies of Ampicillin with *S. aureus Gyrase*

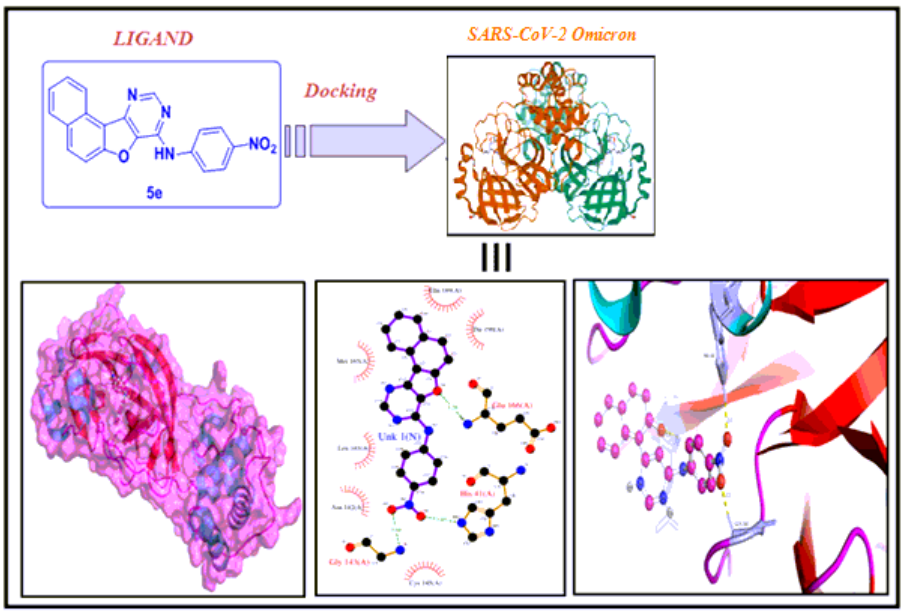

Figure 10

Docking studies of compound 5e with *SARS-CoV-2 Omicron*

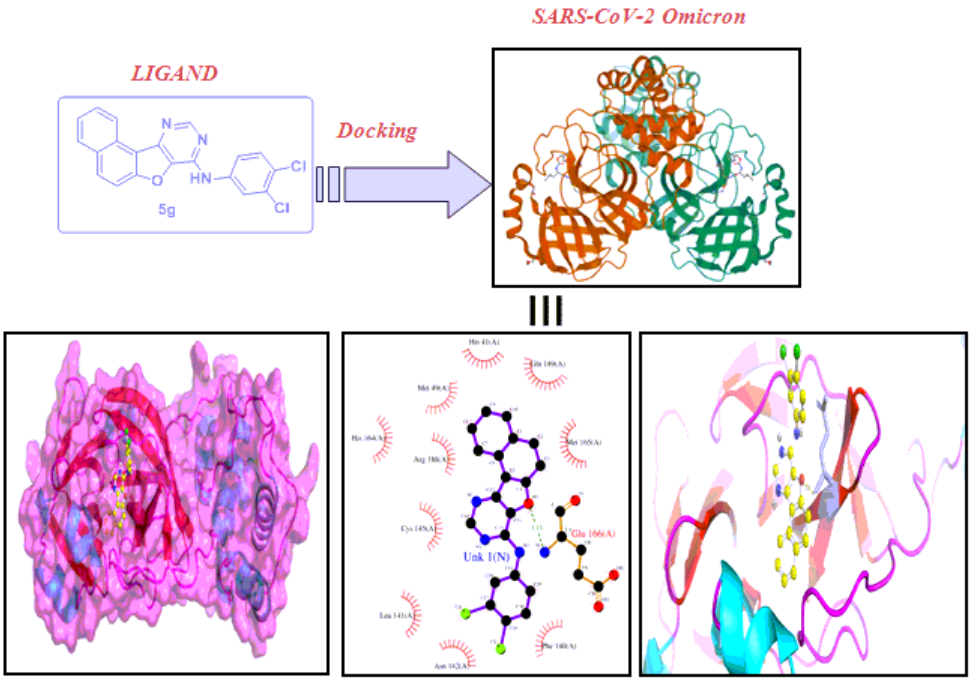

Figure 11

Docking studies of compound 5g with *SARS-CoV-2 Omicron*

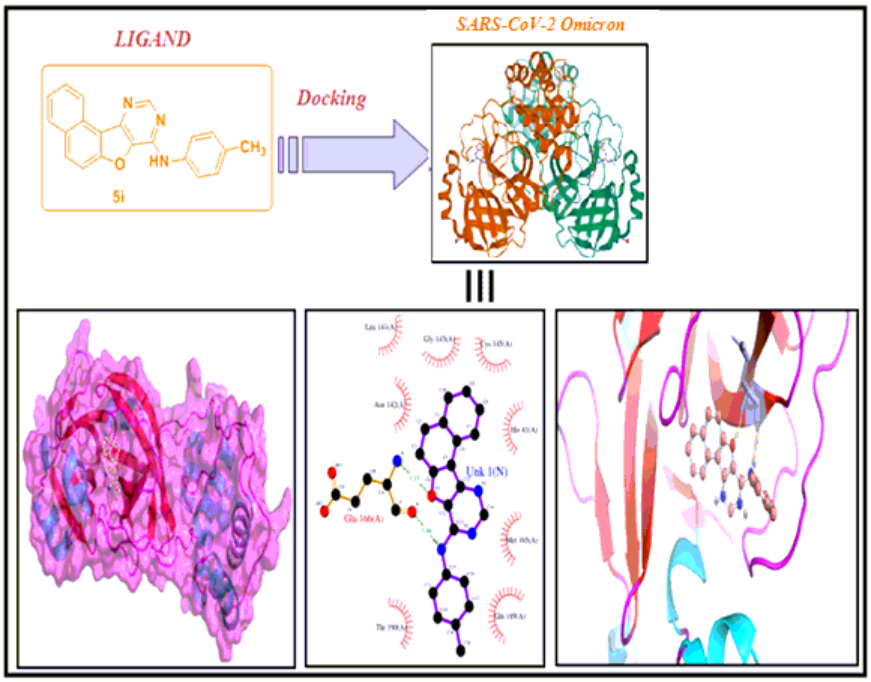

Figure 12

Docking studies of compound 5i with *SARS-CoV-2 Omicron*

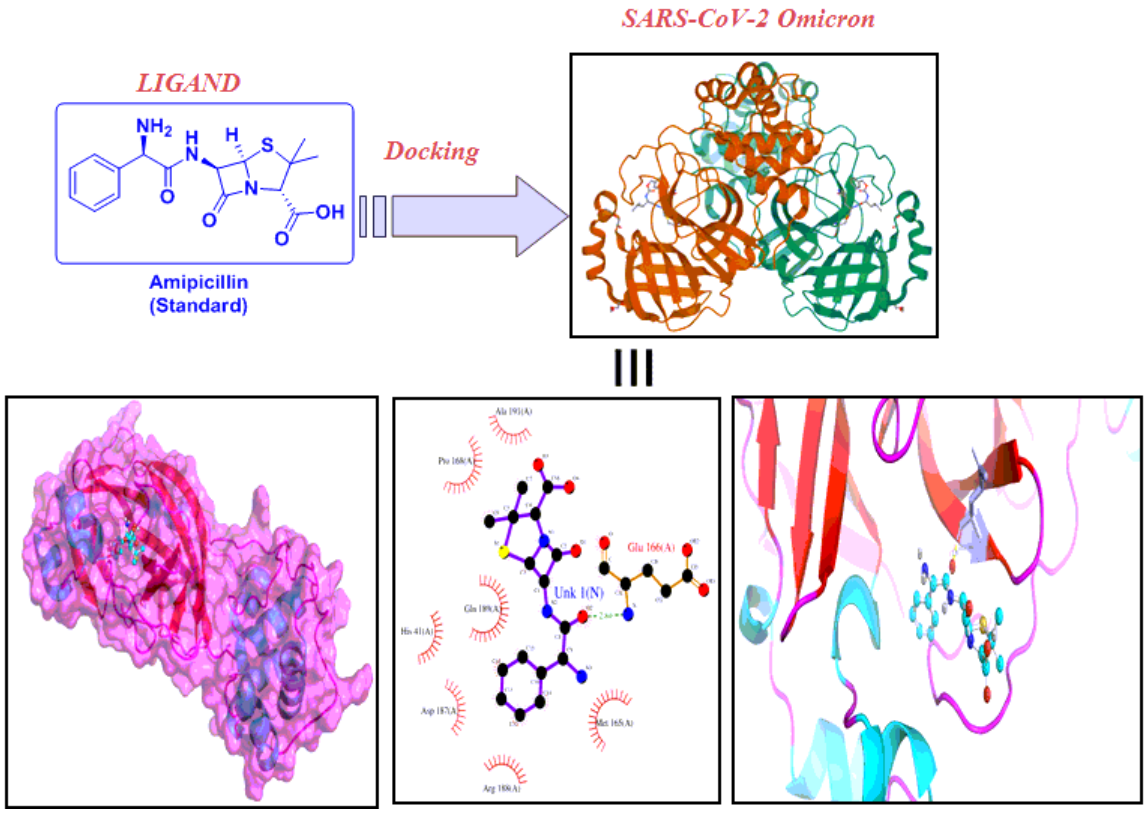

Figure 13

Docking studies of compound Ampicillin with *SARS-CoV-2 Omicron*

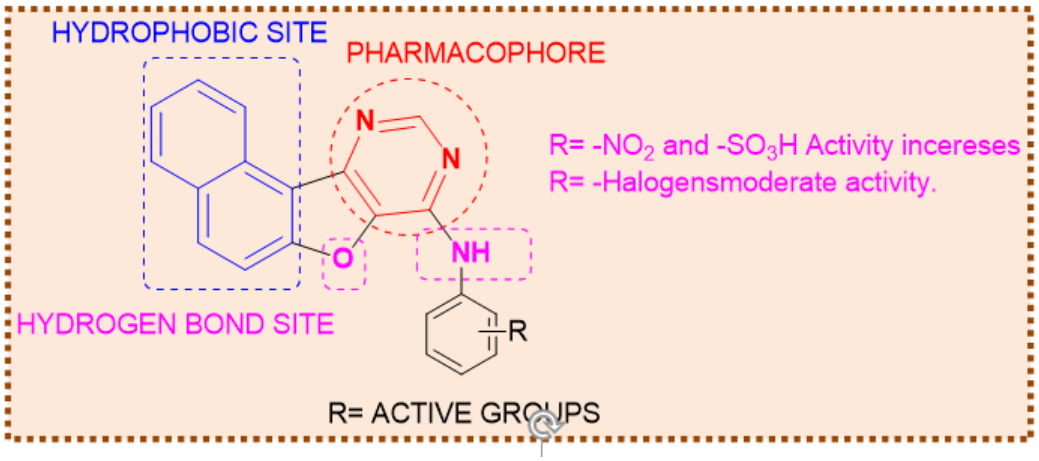

Figure 14

Figure-11: The brief SAR study for synthesized napthofuran-pyrimidines

Supplementary Files

This is a list of supplementary files associated with this preprint. Click to download.

- Supplimentorymaterialnew.pdf
- Scheme1.png